

Optimization of Vapor Post-Deposition Processing for Evaporated CdS/CdTe Solar Cells

B. E. McCandless¹, I. Youm², and R. W. Birkmire
Institute of Energy Conversion
University of Delaware
Newark, DE 19716-3820, USA

¹ Corresponding author.

² Fulbright Visiting Scholar from Department of Physics, Faculty of Science, U.C.A.D, Dakar-Fann, Senegal.

Summary: The effects of thermal annealing in conjunction with CdCl₂ vapor heat treatment on the properties of CdTe/CdS thin films and devices deposited by physical vapor deposition are reported. Results are compared for three treatment variations: high temperature anneal only, high temperature anneal followed by CdCl₂ vapor heat treatment, and CdCl₂ vapor heat treatment only. X-ray diffraction, transmission electron microscopy, and scanning electron microscopy show improved crystallographic properties of the CdTe film and reduced CdS-CdTe interdiffusion when a high temperature anneal is used prior to CdCl₂ treatment. CdTe/CdS solar cells fabricated using an anneal at 550°C in argon prior to the CdCl₂ vapor heat treatment exhibited improved electrical characteristics compared to cells fabricated with no anneal step, yielding V_{oc} exceeding 850 mV.

INTRODUCTION

Polycrystalline thin-film CdTe has shown considerable promise for terrestrial photovoltaic applications due to its near-optimum bandgap, high absorption coefficient, and relative ease of film formation. Thin-film CdTe/CdS cells with efficiencies greater than 10% have been demonstrated using CdTe deposited by a variety of techniques over a wide range of deposition temperatures [1,2]. Physical vapor deposition (PVD) is an ideal deposition technology for separating temperature and chemical effects in the CdS-CdTe structure by allowing chemically pure, single phase CdTe films to be deposited at relatively low temperatures, less than 300°C. Obtaining high conversion efficiencies from such films requires optimization of post-deposition treatment, including exposure of the structure to CdCl₂ and O₂ at temperatures around 400°C. This treatment promotes grain growth within both CdTe and CdS layers and interdiffusion between CdTe and CdS resulting in formation of Cd(TeS) alloys at the interface [3-6]. Under conditions of high oxygen or chloride

concentration, excessive interdiffusion depletes a significant portion of the CdS film thickness [6]. When very thin CdS window layers, $d < 100$ nm, are employed, the post-deposition treatment can consume the entire CdS film. This leads to junctions between the resulting $\text{CdTe}_{1-x}\text{S}_x$ absorber layer and the transparent conductive oxide (TCO) layers, which typically yield much lower V_{oc} and FF. Earlier studies showed that without CdCl_2 , high temperature treatment in air, above 500°C , without CdCl_2 results in working devices, but these devices exhibited low V_{oc} and FF due to insufficient doping of the CdTe layer and formation of surface oxides [7].

In this work, it is shown that use of a high temperature anneal (HTA) prior to CdCl_2 treatment improves the crystallographic properties of the CdTe/CdS films, reduces interdiffusion between CdS and CdTe, and yields cells having V_{oc} greater than 850 mV, which is 20 to 30 mV higher than has been obtained without the anneal step. The reduced interdiffusion offers an additional degree of control over final CdS thickness and may permit use of ultra-thin CdS films in low-temperature deposition processes to obtain high efficiencies. The optimal treatment time is temperature dependent and suggests that rapid thermal annealing near 650°C to 700°C coupled with a short CdCl_2 vapor treatment could be employed to fabricate state-of-the-art devices with CdTe/CdS films deposited at low temperatures.

EXPERIMENTAL

The devices were fabricated in a superstrate configuration on Corning 7059 glass coated with a 200 nm thick $\text{In}_2\text{O}_3:\text{Sn}$ (ITO) layer. CdS films from 180 to 210 nm thick were deposited at 220°C and $3 \text{ \AA}/\text{s}$ from high purity CdS powder. Prior to CdTe deposition the CdS/ITO/glass structures were treated in CdCl_2 vapor at 420°C in air for 15 minutes. This treatment restructures the CdS layer, making it resistant to Te diffusion [8]. CdTe films 2.5

and 5 μm thick were deposited onto the treated CdS at 275 °C and 40 $\text{\AA}/\text{s}$ from 99.999% purity CdTe powder.

After CdTe deposition, three treatment variations were utilized: high temperature anneal (HTA) only; CdCl₂ treatment only; and HTA followed by CdCl₂ treatment. The HTA was carried out in a horizontal tube furnace at temperatures from 500 °C to 580 °C for 10 to 60 minutes. For shorter treatment times, a radiatively heated reactor with graphite susceptors was employed, allowing time resolution of ~30 seconds. In either system, prior to treatment, the treatment chamber was evacuated to 50 m Torr and backfilled with the desired ambient gas: argon for the HTA and a mixture of argon and oxygen for the CdCl₂ vapor treatment. The CdCl₂ vapor treatments were carried out in a reactor configured to deliver CdCl₂ vapor at a partial pressure of 5-10 m Torr to the CdTe surface at ~420 °C for 20 minutes [9].

The structures were characterized by optical microscopy (OM), scanning electron microscopy (SEM), energy dispersive x-ray spectroscopy (EDS), transmission electron microscopy (TEM), and x-ray diffraction (XRD). Optical transmission and reflection were made using a Perkin-Elmer Lambda-9 spectrometer. Measurements were made from 400 to 900 nm in 2 nm steps to assess relative shifts in the location of the CdTe absorption edge. SEM and OM images were analyzed by the method of Heyn [10] to determine average grain size. Selected samples were etched in a solution of K₂Cr₂O₇:H₂SO₄ to reveal grain boundaries and to verify the identification of surface features as grains.

Wide-angle $\theta/2$ XRD scans were made with a Philips/Norelco powder diffractometer using Cu k x-rays to determine degree of preferred orientation and bulk lattice parameter of grains oriented normal to the substrate plane. XRD data was stripped of $\theta/2$ components using the Rachinger correction [11] and smoothed prior to analysis. The degree of

preferred orientation in the films was calculated from the $\frac{1}{N}$ peak intensities of the broad scans using the method of Harris for polycrystalline fiber texture analysis [12]. This method estimates the probability of finding an (hkl) plane lying parallel to the substrate. For the (111) reflection, the orientation parameter, $p(111)$, is obtained by normalizing to the random powder pattern for the number of peaks, N , being analyzed. If $p(111) = N$, all the grains of the films are oriented in the $\langle 111 \rangle$ direction normal to the substrate; $p(111) = 1$ indicates random grain orientation; and $p(111) < 1$ indicates preferred orientation along an axis other than $\langle 111 \rangle$. Nine peaks were considered for each sample, $p(111) = 9$ indicates that the film is completely (111) oriented.

The lattice parameter of the top portion of the treated CdTe layer was obtained by extrapolation of individual (hkl) lattice parameters using the Nelson-Riley-Sinclair-Taylor function [13, 14]. The reduction applies only to the top $\sim 3 \mu\text{m}$ of the $5 \mu\text{m}$ thick CdTe films because of attenuation of the Cu k x-rays in CdTe.

Narrow-angle XRD patterns of individual peak profiles such as the (511)/(333) were obtained to assess the crystallographic quality of the CdTe film and the distribution of S within the CdTe layer after treatment. The peak profiles were obtained under conditions of constant count to increase the signal to noise ratio and sensitivity to underlying regions of compositional deviation from pure CdTe as shown in Reference [6]. For the (511)/(333) reflection with Cu k x-rays, located near 76° , the detection of diffracted x-rays is limited to a depth of approximately $3 \mu\text{m}$ into the CdTe film. To permit detection of the interfacial region, samples were thinned to $\sim 2 \mu\text{m}$ by etching in a weak solution of bromine-methanol.

Cross-sectional transmission electron microscopy with a Philips EM400T microscope was used to evaluate the crystal quality of individual grains and the integrity of the CdTe-CdS

interface after the treatments. Samples were prepared by cutting slabs from the structure, mechanically polishing to 10 μm lateral thickness, followed by ion-milling at 5 kV to electron transparency thicknesses using a Gatan Dual ion mill.

Back contacts were formed on the CdTe surface by evaporating 15 nm of Cu followed by heat treatment at 180°C in argon for 30-40 minutes and then etching the structure in $\text{Br}_2:\text{CH}_3\text{OH}$ solution to remove metallic Cu as described in reference [15]. Devices were fabricated by etching, applying carbon paste electrodes, and scribing. Device performance was characterized by current-voltage (J-V) measurements performed at 25°C under AM 1.5 simulation at 100 mW/cm^2 .

RESULTS AND DISCUSSION

Materials Characterization

SEM and optical microscopy revealed an increase in lateral CdTe grain size after all treatments. EDS measurements of the 5 μm thick films at 20kV revealed no detectable changes in surface stoichiometry after any of the treatments. Changes in grain size, orientation, lattice parameter, and optical bandedge are listed in Table 1. The as-deposited CdTe layers grown on CdS/ITO/glass exhibit a faceted structure with lateral grain size of $\sim 0.2 \mu\text{m}$. After CdCl_2 treatment only, the film surface consisted of rounded grains with penetrating boundaries (Figure 1a) and an average grain size of $\sim 3 \mu\text{m}$. The high temperature anneal also promoted grain growth, but to a lesser extent as shown in Table 1. A subsequent CdCl_2 heat treatment further increased the grain size, resulting in planar surface morphology and lateral grain size of $\sim 5 \mu\text{m}$, with maximum grain size up to 7 μm suggesting dramatic reduction of the grain boundary volume (Figure 1b).

Recrystallization is also indicated by the XRD measurements. In Table 1, the as-deposited CdTe/CdS/ITO/glass structure shows strong (111) preferred orientation with $p(111)$ of 6 to 7. The HTA promoted a more randomized structure with $p(111)$ in the range from 1 to 3. CdCl₂ treatment also randomized the crystallographic orientation. These texture changes indicate dramatic atomic rearrangement in the CdTe layer in response to high temperature with no chloride and at low temperature in the presence of chloride.

The lattice parameter of annealed CdTe powder was measured to be 6.480 to 6.481 Å. Lattice parameter determinations of the 5 μm thick CdTe films show that as-deposited CdTe films are slightly strained, having lattice parameters greater than expected for CdTe, in the direction perpendicular to the substrate plane. This could arise from compressive shear strain in the substrate plane arising from heteroepitaxial growth of CdTe on CdS [6]. High temperature annealing relieves this strain, shifting the lattice parameter close to the expected value for pure CdTe. In previous work[15], CdCl₂ heat treatment was shown to promote interdiffusion between CdS and CdTe shifting the lattice parameter to even lower values by formation of CdTe_{1-x}S_x. In Table 1 of this work, the lattice parameter of heat treated 5 μm thick films deviates from the pure CdTe value only for the sample receiving CdCl₂ treatment with no HTA, indicating less penetrating diffusion of CdS into CdTe when the HTA is used in conjunction with the CdCl₂ treatment.

The primary effect of the high temperature step is annealing of defects which act as diffusion paths. Table 1 shows that for the bulk of the film, the HTA alone reduced intermixing and did not produce a significant increase in lateral grain size. The reduction in bulk lattice parameter to that of pure CdTe suggests relief in tensile strain perpendicular to the substrate by reduction in compressive forces at the film interface. The value of the lattice parameter indicates low CdS incorporation through the top 3 μm of the film. However, CdS-CdTe interdiffusion within the grains at the interface did produce a

CdTe_{1-x}S_x layer which was detected by the reduced bandgap in HTA treated films. It has been suggested that formation of the CdTe_{1-x}S_x interlayer reduces structural defects that arise due to lattice mismatch between CdS and CdTe [16-18], leading to improvement in CdTe cell performance. Therefore, an attempt was made to investigate the interface condition of the cells fabricated with different post-deposition processing. This was accomplished by combining the results of narrow-angle XRD scan of thinned samples, optical absorption measurements, and TEM images of cross-sections.

Figure 2 shows XRD profiles of the CdTe (511)/(333) peak for treated and thinned 2 μm films for three treatment cases: a) after the HTA at 550°C for 30 minutes; b) after CdCl₂ treatment at 420°C for 20 minutes; and c) after both treatments. The profile after the HTA is symmetrical (Figure 2a), but is broader than the instrumental value, FWHM = 0.12 degree. The CdCl₂ treatment alone produced a broad asymmetrical peak with a tail extending towards higher angle (lower d-spacing), indicative of significant alloying with CdS (Figure 2b). Combining the two treatments, however, resulted in a narrow symmetrical peak, indicating a low degree of CdTe-CdS alloying and good crystallinity (Figure 2c).

The optical absorption coefficient (α) squared versus energy is shown in Figure 3 for an as-deposited and three treated structures having a 2.5 μm thick CdTe layer. The corresponding shift in the bandedge, taken at α² = 9 x 10⁸ cm⁻¹, is listed in Table 1. The absorption shift was measured on 2.5 μm CdTe/0.2 μm CdS to maximize sensitivity in the high diffusion region of the structure. For the as-deposited film, the bandedge is located at ~1.53 eV. Annealing at 550°C for 30 minutes reduced the bandedge location by 15 meV with no further reduction after CdCl₂ heat treatment. Treatment with CdCl₂ alone, however, shifted the absorption edge by 25 meV, exactly as reported in reference [6], in which the shift, E_g, has been correlated with CdS-CdTe alloying. Taking the shift of the edge to represent the degree of interfacial CdTe-CdS alloying, it is again concluded that the CdCl₂ treatment alone

resulted in the largest degree of CdS diffusion and alloying, while the HTA alone or the combination treatment resulted in less alloy formation. From this data alone, the spatial extent of and the distribution within the intermixed, high diffusion region cannot be determined.

Figure 4 shows TEM images of the CdTe-CdS interface after the CdCl₂ treatment and after the combined HTA and CdCl₂ treatment. No data is available for the HTA alone case. The CdCl₂ treatment alone produced large grains, but with boundaries lying at all angles to the interface. Also, the CdS layer was completely consumed by interdiffusion in some regions and thinned in others. Combining the HTA and CdCl₂ treatment, however, resulted in only perpendicular grain boundaries and a continuous CdS layer as shown in Figure 4c.

Thus, the combined measurements show that some degree of interfacial mixing occurs during all treatments. The CdCl₂ treatment alone produces the greatest degree of mixing, evidenced by the measurable reduction in lattice parameter, the presence of a high-angle XRD alloy tail, the greatest shift in the CdTe bandedge, and the complete loss of portions of the CdS layer in the TEM images. The diffusion process in this case proceeds rapidly due to the high grain boundary volume and via other crystallographic defects that exist at the moment that chloride species reach the junction, resulting in CdS loss from the window layer and incorporation into the absorber layer as CdTe_{1-x}S_x. The HTA step, by partially recrystallizing the CdTe layer, reduces diffusion pathways, resulting in a slower CdS-CdTe diffusion process during subsequent chloride treatment. This results in a more chemically uniform absorber layer and offers a degree of control over the interdiffusion process. In CdCl₂ treatment, simply heating the substrate prior to heating the CdCl₂ source is also effective at reducing intermixing compared to unison heating of thin-film samples and source [9].

Devices

The device results for the structures treated under various conditions are listed in Table 2.

The primary influence of the HTA step when combined with the CdCl_2 treatment is on the V_{oc} of the devices, which exceeded 850 mV, which is comparable to state-of-the-art devices deposited at high temperatures and receiving a CdCl_2 treatment [20]. Using the HTA alone yielded only 3.9 % efficiency while the CdCl_2 treatment alone yields ~11% efficiency.

Using the HTA prior to CdCl_2 treatment was found to yield comparable or higher efficiency, up to 12% for a range of conditions, with optimal results obtained at 550°C for 30 minutes. Shorter treatment times can be employed by increasing the temperature as shown for samples in the last group, although the V_{oc} is lower. Noteworthy is the sample treated at 600°C for 4 minutes followed by a 10 minute CdCl_2 treatment, yielding baseline performance. This suggests that an appropriate temperature-time profile can be established for reducing overall processing time.

A possible explanation of V_{oc} enhancement for the device with the HTA step at 550°C is lower saturation current via reduction of recombination centers in the junction. Such centers could arise from residual crystallographic defects in the CdTe which are not removed by the 420°C CdCl_2 heat treatment alone. At this temperature, an ideal balance is obtained between defect annealing and interdiffusion. The fill factors exhibited in Table 2 are less than optimal due to high series resistance; R_{sc} values for these devices ranged from 6 to 10 $\Omega \cdot \text{cm}^2$ and are believed to be related to contact resistance at the back of the device.

CONCLUSIONS

The advantages of employing a high temperature anneal prior to CdCl₂ heat treatment of physical vapor deposited CdTe/CdS films have been shown. Structural and morphological characterization of the CdTe/CdS structures have highlighted progressive recrystallization, grain growth, and interdiffusion. Interdiffusion between CdS and CdTe occurs during both the HTA and the CdCl₂ heat treatment, but is least for structures treated with the HTA step prior to the CdCl₂ treatment. This offers a method for retarding CdS diffusion into CdTe for low-deposition temperature processes.

For evaporated CdTe/CdS films deposited at moderately high growth rate and low substrate temperature, the vapor treatment process combined with an anneal step at 550°C yielded V_{oc} exceeding 850 mV, which is comparable to state-of-the-art-devices deposited at high temperatures. However, the efficiency of these devices is limited by the short circuit current density and fill factor, which can be improved by employing thinner CdS layers and by contact optimization, respectively. Use of an anneal at 600°C with a shorter CdCl₂ treatment resulted in baseline 10-11% efficiency which offers a pathway for reduced total processing time. The higher V_{oc} , reduced intermixing, and improved crystallographic properties appear to be coupled for the PVD films and offers an explanation for the apparent discrepancy in conversion efficiency between high (>500°C) and low (<500°C) temperature CdTe fabrication processes in use today.

ACKNOWLEDGMENTS

The authors would like to thank S. Fields, K. Hart, and J. Yu for fabricating and treating the samples. We thank C-Y. Ni for making the TEM measurements and W. N. Shafarman for helpful discussions. One of the authors (I.Y.) is grateful to USAI (Fulbright program) for

scholarship, to IEC for hospitality and to the Department of Physics, U. C. A. D. for leave of absence. This work was supported by NREL subcontract No. XAV-3-13170-01.

REFERENCES

1. D. Bonnet, *Int. J. Solar Energy*, **12**, 1-14 (1992).
2. T. L. Chu and S. S. Chu, *Int. J. Solar Energy*, **12**, 121- 132 (1992).
3. R. W. Birkmire, J. E. Phillips, W. A. Buchanan, S. S. Hegedus, B. E. McCandless, W. N. Shafarman and T. A. Yokimcus, *Annual Report of NREL Subcontract XAV-3-13170-01*, NREL, Golden, CO (1994).
4. N. Nakayama, T. Arita, T. Aramoto, T. Nisho, H. Higuchi, K. Omura, K. Hiramatsu, N. Ueno, M. Murozono and H. Takakura, *Sol. Energy Mater. and Solar Cells*, **35**, 271-278 (1994).
5. M. Özsan, D. R. Johnson, D. W. Lane and K. D. Rogers, *Proc. 12th European Photovoltaic Solar Energy Conf.*, Amsterdam, 1600-1603 (1994).
6. B. E. McCandless, L. V. Moulton, and R. W. Birkmire, *Progress in Photovoltaics: Research and Applications*, **5**, 249-260 (1997).
7. R. W. Birkmire, B. E. McCandless and W. N. Shafarman, *Solar Cells*, **23**, 115-126 (1988).
8. R. W. Birkmire, B. E. McCandless and S. S. Hegedus, *Int. J. Solar Energy*, **12**, 145-154 (1992).
9. B. E. McCandless, H. Hichri, G. Hanket, and R. W. Birkmire, *Proc. 25th IEEE Photovoltaic Specialist Conf.*, 781 (1996).
10. S. H. Avner, *Introduction to Physical Metallurgy*, McGraw-Hill, New York, 102-104 1974.
11. W. A. Rachinger, *Jour. Sci. Inst.*, **25**, 254 (1948).
12. G. B. Harris, *Phil. Mag.* , **43**, 113 (1952).

13. J. B. Nelson and D. P. Riley, *Proc. Phys. Soc.*, London, **57**, 160 (1945).
14. A. Taylor and H. Sinclair, *Proc. Phys. Soc.*, London, **57**, 126 (1945).
15. B. E. McCandless and R. W. Birkmire, *Solar Cells*, **31**, 527-535 (1991).
16. I. Clemmick, M. Burgelman, M. Casteleya, J. De Porter and A. Veravet, *Proc 22nd IEEE Photovoltaic Specialist Conf.*, 1114-1119 (1991).
17. D. Mao, L. H. Feng, Y. Zhu, J. Tang, W. Song, R. Collins, D. L. Williamson and J. U. Trefny, *AIP Conf. Proc.*, **353**: *13th NREL Photovoltaic Program Review*, Lakewood, CO, 1995, 352-359, AIP Press, Woodbury 1996.
18. Z. C. Feng, H. C. Chou, A. Rohatgi, G. K. Lim, A. T. T. S. Wee and K. L. Tan, *J. Appl. Phys.*, **79**, 2151-2153 (1996).
19. A. L. Fahrenbruch and R. H. Bube, *Fundamentals of Solar Cells*, Academic Press, New York 1983.
20. A. Rohatgi, *Int. J. Solar Energy*, **12**, 37- 49 (1992).
21. C. Ferekides, J. Britt, Y. Ma and L. Kettian, *Proc 23rd IEEE Photovoltaic Specialist Conf.*, 389-393 (1993).

Table 1: Values of average grain size, orientation parameter, lattice parameter, and absorption edge shift for CdTe films before and after processing. The grain size, orientation parameter, and lattice parameter are for 5 μm CdTe, and the absorption shifts are for 2.5 μm CdTe.

Sample condition	Average Grain Size ($\pm 0.1 \mu\text{m}$)	p(111)	a_0 ($\pm 0.001 \text{ \AA}$)	E (eV)
As-deposited	0.2	6.2	6.492	0
HTA 550°C, 10' only	0.3	2.3	6.478	15
HTA 550°C, 30' only	0.8	1.9	6.479	15
HTA 580°C, 10' only	0.5	1.0	6.480	15
HTA 550°C, 30' + CdCl ₂ 420°C, 20'	5.0	2.3	6.480	15
CdCl ₂ 420°C, 20' only	3.0	1.0	6.476	25

Table 2: Device results for different processing conditions under AM 1.5 illumination.

Processing Conditions		V_{oc} (mV)	J_{sc} (mA/cm ²)	FF (%)	(%)
No HTA	CdCl ₂ 420°C, 20'	800	21	65	10.9
HTA 550°C, 30'	No CdCl ₂	625	16.4	38.3	3.9
HTA 550°C, 10'	CdCl ₂ 420°C, 20'	834	19.6	64.4	10.5
HTA 550°C, 30'	CdCl ₂ 420°C, 20'	853	21.0	66.9	12.0
HTA 550°C, 45'	CdCl ₂ 420°C, 20'	831	19.8	67.5	11.1
HTA 550°C, 60'	CdCl ₂ 420°C, 20'	733	21.9	54.0	8.7
HTA 580°C, 10'	CdCl ₂ 420°C, 20'	814	19.8	66.5	10.7
HTA 580°C, 30'	CdCl ₂ 420°C, 20'	774	18.6	54.4	7.8
HTA 600°C, 4'	CdCl ₂ 420°C, 20'	793	20.2	69.6	11.1
HTA 600°C, 4'	CdCl ₂ 420°C, 10'	751	21.9	65.0	10.7
HTA 600°C, 15'	CdCl ₂ 420°C, 20'	789	21.7	70.6	12.1

FIGURES

1. SEM photograph of CdTe surface: a) after CdCl₂ treatment at 420°C for 20 minutes in air and b) after HTA at 550°C for 30 minutes in argon followed by CdCl₂ treatment at 420°C for 20 minutes in air.
2. X-ray diffraction profiles of CdTe (511)/(333) peak: a) after HTA at 550°C for 30 minutes in argon; b) after CdCl₂ treatment at 420°C for 20 minutes in air; and c) after HTA followed by CdCl₂ treatment.
3. Optical absorption coefficient squared versus energy of 2.5 μm thick CdTe/0.2 μm CdS: a) as-deposited; b) after HTA at 550°C for 30 minutes in argon; c) after HTA followed by CdCl₂ treatment at 420°C for 20 minutes in air; and d) after CdCl₂ treatment at 420°C for 20 minutes in air alone.
4. TEM cross-section images of CdTe/CdS interface: a) after CdCl₂ treatment at 420°C for 20 minutes in air; b) same sample but at higher magnification; and c) after HTA at 550°C for 30 minutes followed by the same CdCl₂ treatment.

Figure 1.

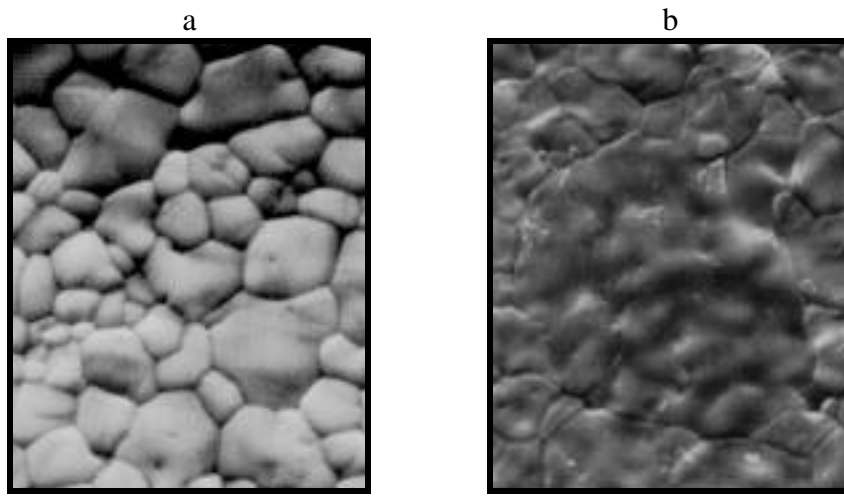
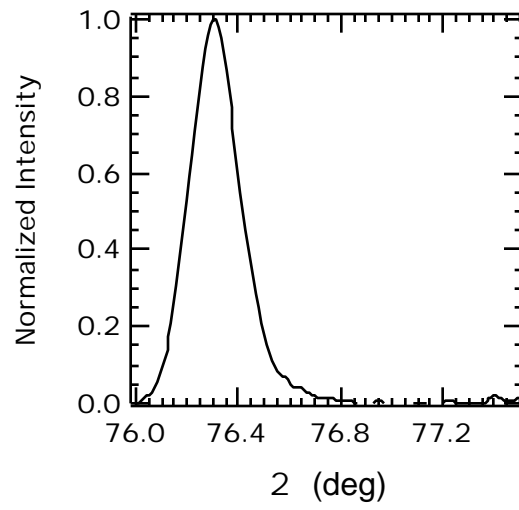
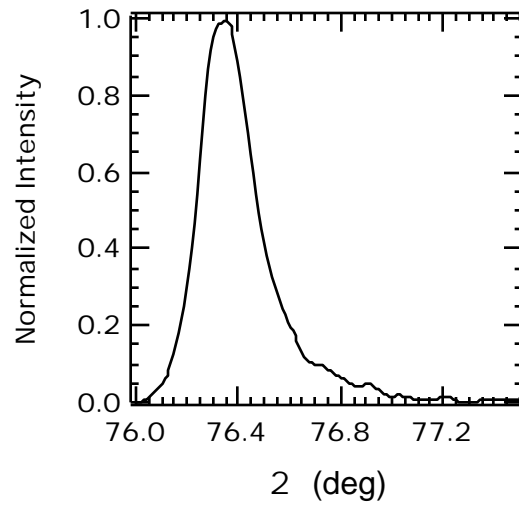


Figure 2a.



b.



c.

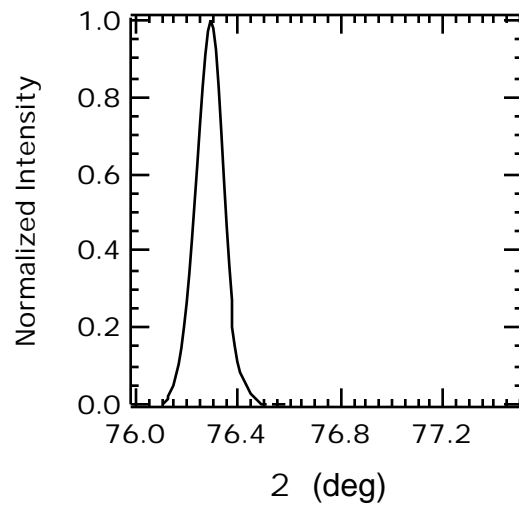


Figure 3.

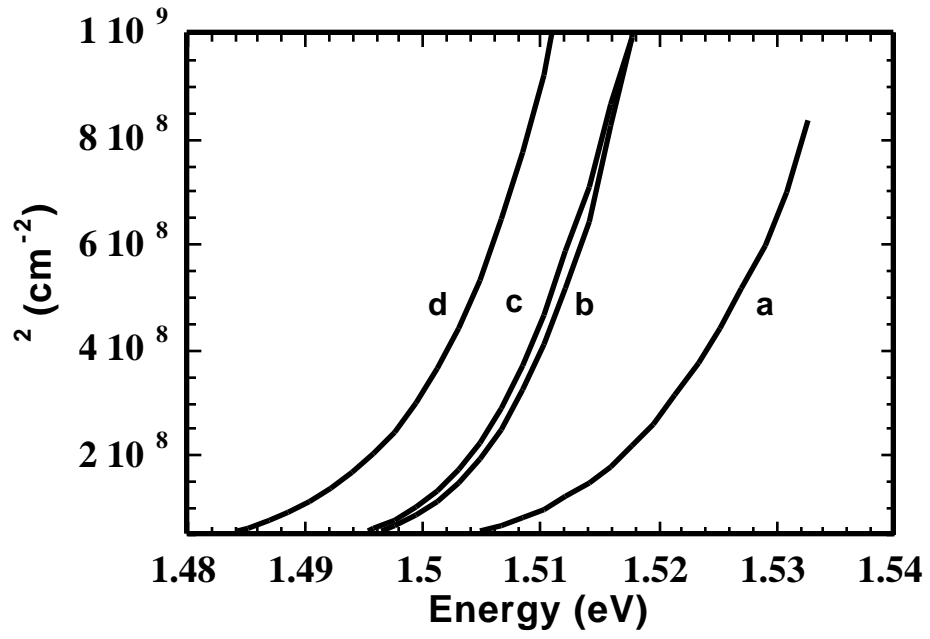


Figure 4.